Short-term circulating tumor cell dynamics in mouse xenograft models and implications for liquid biopsy.

Amber Williams[1], Jessica Fitzgerald[1], and Mark Niedre[1]*

[1]Northeastern University, Department of Bioengineering, Boston, MA, 02115

*Corresponding author at m.niedre@neu.edu

Abstract:

Motivation: Circulating tumor cells (CTCs) are important in hematogenous cancer metastasis, and are usually studied by isolation from small peripheral blood samples. However, little is known about the short-term dynamics of CTC *in vivo*.

Methods: We recently developed an instrument called 'diffuse *in vivo* flow cytometry' (DiFC), that allows counting of fluorescently-labeled circulating cells without drawing blood samples. DiFC samples 50μL of circulating peripheral blood per minute, allowing continuous, non-invasive detection of CTCs. We used DiFC to study short-term changes in CTC numbers over time in mouse xenograft models of Lewis Lung carcinoma (LLC) and multiple myeloma (MM), in intervals corresponding to approximately 1, 5, 10 and 20% of the peripheral blood volume.

Results: For rare CTCs (LLC), short intervals (small blood volumes) frequently yielded no CTC detections, even when metastatic disease was present. For more abundant CTCs (MM), quantitative estimation of CTC numbers with single small blood volumes was generally highly inaccurate. Moreover, the observed variability in CTC detections in blood volumes often exceeded that predicted by Poisson statistics, suggesting that the mean number of CTCs changes over the timescale of minutes.

Conclusions: Overall, CTC numbers were observed to be highly dynamic *in vivo* over the course of 35-65 minute DiFC scans. These data provide direct experimental evidence of the notion that detection and quantitation accuracy can be improved by analysis of larger blood volumes, or by in vivo detection methods. In addition, quantitative accuracy can be improved by averaging multiple small blood samples taken over time, as opposed to single larger blood samples.

Keywords: circulating tumor cells, dynamics, optical devices, fluorescence, liquid biopsy

1. Introduction

Circulating tumor cells (CTCs) are of great interest in cancer research due to their importance in hematogenous cancer metastasis. CTCs shed from tumors into the peripheral blood (PB), a small number of which may form metastases. It is these metastases that are extremely difficult to control clinically, and eventually result in 90% of cancer-related deaths [1, 2]. As such, CTCs are highly studied both clinically and in pre-clinical small animal models. The vast majority of these studies involve "liquid biopsy" techniques, wherein CTCs are isolated in fractionally small blood samples [3, 4]. While it has been clearly established that elevated CTCs in patient blood samples is associated with reduced overall survival for major cancers such as breast [5], colorectal [6], and prostate [7], the clinical value of CTC enumeration (beyond detection) is still unclear [8-11]. One major known challenge with liquid biopsy includes the heterogeneity of CTCs, leading to increased efforts for molecular and genetic characterization of individual CTCs after isolation [12-14].

A less studied challenge is with respect to quantification accuracy: liquid biopsy implicitly assumes that the number of CTCs in small blood samples is representative of the whole peripheral blood volume (PBV). Several researchers have shown that this assumption may be dubious, due to the rarity of CTCs in the blood, the fractionally small volume of blood samples relative to the total PBV, and the expected statistical variability in detection events [15, 16]. The only FDA cleared method for enumerating CTCs clinically is currently CellSearch, which is used to analyze 7.5 mL blood samples, or about 0.015% of the approximately 5L human PBV [6, 17, 18]. Other experimental microfluidic platforms typically analyze similarly small blood volumes, usually in the range of 2-10 mL [19-21]. In pre-clinical mouse studies, blood collection is typically limited to 100-200 μL of blood every two weeks, or about 5-10% of the approximately 2mL mouse PBV [22, 23]

As such, if sufficiently rare, CTCs may not be detected, even if metastatic disease is present. For instance, Maestro et. al. found that only 62.3% of patients with metastasized epithelial cancers had at least 1 CTCs in 7.5mL samples over the detection limit [24]. Moreover, most theoretical treatments of the problem assume that CTC detection statistics should follow a Poisson distribution [15, 25], which further assumes that CTCs are well mixed in the blood, and that the average number of CTCs in circulation does not change significantly over the short-term (minutes, hours or days surrounding the blood draw).

'*In vivo* flow cytometry' (IVFC) is a general term for optical instrumentation designed to enumerate circulating cells directly in vivo, most often by fluorescence or photoacoustic methods [23, 26]. We recently developed 'diffuse in vivo flow cytometry' (DiFC), which is a fluorescence-based, small animal research instrument specifically developed for enumerating extremely rare (less than 1 cell per mL) cells circulating in the peripheral blood (PB) [27-30]. DIFC uses highly scattered light to sample large blood volumes in

large veins and arteries. The main advantage of DiFC compared to microscopy-IVFC is therefore sensitivity, in that it samples at least an order of magnitude more circulating blood per unit time (50 μL versus 1 μL of blood per minute) [23]. We recently used DiFC to monitor CTC dissemination during disease development in mouse xenograft models of multiple myeloma (MM) and Lewis lung carcinoma (LLC) [30, 31].

Until now, we used DiFC to measure only the *time-averaged* (mean) number of CTC in circulation on a given day, but did not consider the *short-term* dynamics of CTC detections which varied significantly on the timescale of seconds or minutes. These short-term variations are not observable by drawing blood samples (liquid biopsy), and are therefore uniquely measurable with in vivo methods such as DiFC. There is to our knowledge only one previous report studying CTC dynamic fluctuations over time in pre-clinical models with a fluorescence microscopy-based IVFC instrument [32]. In this paper, we studied CTC detection rates in time intervals of 24, 120, 240, and 480 seconds, which correspond to approximately 1, 5, 10, and 20% of the mouse PBV, respectively. We also compared these against in silico data and phantom models with well mixed fluorescent microspheres.

This analysis revealed some interesting observations with insights for the use of small blood samples for the study of CTCs. Overall, DiFC data revealed that CTC numbers are highly dynamic over short-time scales. These data provide direct in vivo confirmation of the notion that use of fractionally small blood samples for estimation of CTC burden is highly sensitive to sampling error, and is generally quantitatively inaccurate [15, 16, 25]. These data also showed that the variability of CTC detection rates often exceeded that predicted by Poisson statistics, suggesting that the CTCs are in general not well-mixed in the peripheral blood. As we discuss, this can be explained by non-constant tumor shedding dynamics, and the short half-life of CTCs in circulation [19, 33].

2. Methods

2.1 DiFC Instrument and Signal Processing

The DiFC instrument and data processing algorithms were described in detail previously [29, 30]. Briefly, two specially designed fiber-optic probes are placed in-line along a major blood vessel (in this case, the ventral side of the tail of a mouse) as shown in ***figure 1a,b***. Fluorescently-labeled CTCs are detected by laser induced fluorescence as they pass through the DiFC field of view (***fig. 1c)***. Integrated filters and collection optics allowed minimization of the non-specific tissue autofluorescence, and detection of weak transient fluorescent peaks from moving cells.

DiFC analysis also uses "peak matching" between the two detection fibers to identify cells moving the in the forward (arterial) or reverse (venous) directions (***fig. 1c)***. As described in Tan 2019, peaks were matched based on their amplitude, temporal width (which is indicative of cell speed through fiber field of view), and temporal delay between channels (speed) [29]. This approach allows us to monitor the count rate in a single blood vessel (in this case the ventral caudal artery) over time, and almost complete elimination of false-positive detections due to e.g. motion artifacts, which do not meet the matching criteria [30]. DiFC detections of arterial CTCs can be visualized using a simplified temporal raster event plot: as shown in ***fig. 1f***, each vertical black line represents a single detection of an arterial CTC in time.

Analysis of DiFC scan intervals and equivalent blood volumes: As such, DiFC data therefore allowed us to observe and analyze the rate of CTC detections continuously over time. We previously calculated that DiFC samples approximately 50 μL per minute [30] of circulating peripheral blood. Central to our analysis here is the assumption that CTC counts in a specific DiFC *time interval* is equivalent to the number of CTCs that would be counted in a *blood sample* of corresponding volume drawn at that time. For example, a 24 s DiFC scan interval is equivalent to approximately 20 μL of blood, or about 1% of the PBV of a mouse. In this work, we considered 24, 120, 240 and 480 s DiFC scan intervals, equivalent to 20, 100, 200 and 400 μL, or about 1%, 5%, 10% and 20% of the PBV.

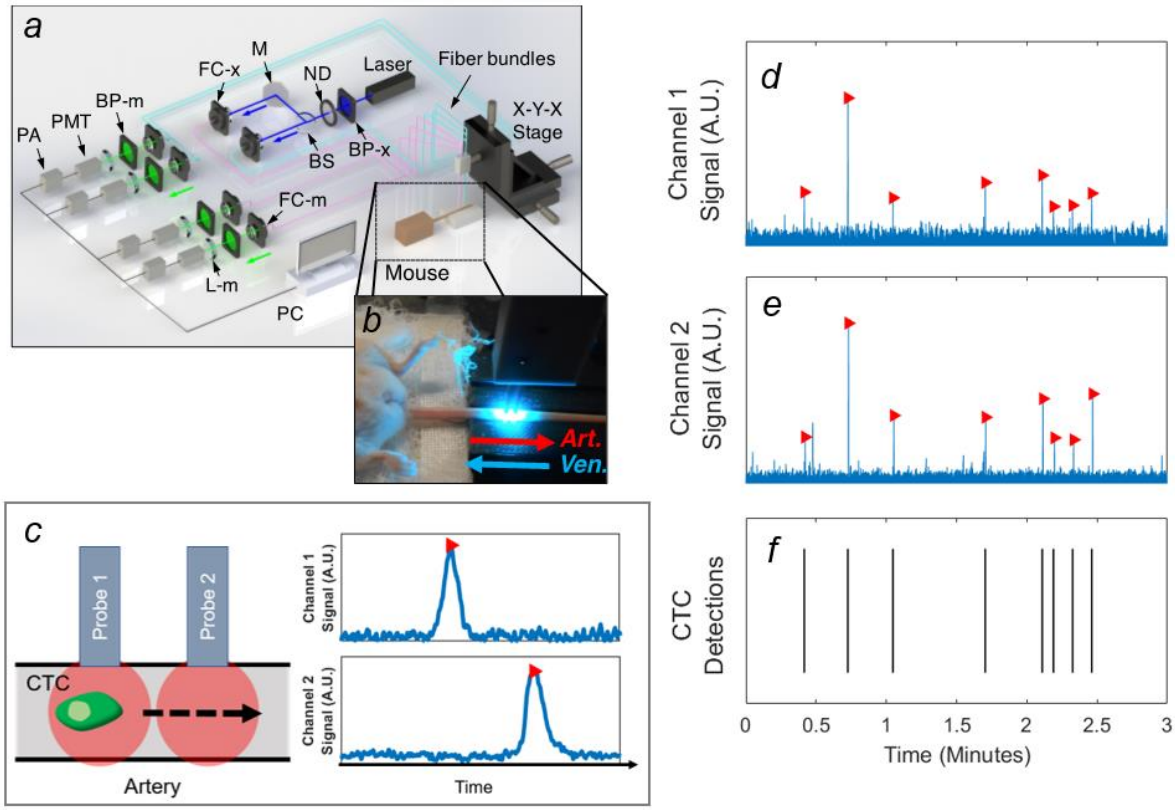

Figure 1. (a) Diagram of DiFC system (with permission from the Journal of Biomedical Optics). (b) Fiber optic probes aligned on the tail of a mouse. (c) Diagram of a CTC passing by the probes and the resulting peaks in both channels of DiFC data that are matched to identify the cell moving in the artery. (d,e) Example set of MM CTC data with peaks matched in the arterial direction. (f) Example raster plot of detected cells (matched peaks) over time.

2.2 DiFC Data Sets

In this work, we analyzed four data sets as follows:

i) Lewis lung carcinoma (LLC) lung metastasis model: We used DiFC to detect CTCs in circulation during LLC development in mice [31]. 10^6 LLC cells (LL/2.GFP.Luc) expressing the green fluorescent protein (GFP) were implanted sub-cutaneously in nude mice (N = 24) and allow to grow for up to 5 weeks after inoculation. DiFC was performed for 40-65 minutes 1-7 times over the course of tumor development. CTCs were observed in circulation as early as 5 days after implantation and generally increased over time. However, as discussed in Fitzgerald et. al. [31], CTCs were exceedingly rare, with detection rates ranging from 0.02 to 1.11 CTCs per minute, or about 0.4 to 22 CTCs per mL. Moreover, they did not in general increase monotonically in time as the primary tumor grew. Rather, CTC numbers changed substantially over the growth, with DiFC scans showing no CTC detections on days following DiFC scans where CTCs were detected. ***Figure 2a-c*** shows example tumor development and varying rates of DiFC detections for one mouse.

<u>ii) Multiple myeloma (MM) disseminated xenograft model:</u> As described in Patil 2019, we also used DiFC to measure CTC dissemination in a MM xenograft model [30]. Briefly, 5 x 10^6 MM.GFP.Luc cells were injected intravenously in SCID mice. Each mouse was scanned with DiFC for 35 minutes, twice weekly up to 5 weeks following inoculation. We also regularly performed Bioluminescence Imaging (BLI) to track disease development. In contrast to the LLC model, MM CTC numbers generally increased over time, and were more abundant. Example DiFC data for one mouse is shown in ***figs. 2d-f***, where an increase in GFP+ CTCs measured in circulation was observed alongside MM burden (BLI). Only data sets where the average count rate was at least 0.5 CTCs per minute were used, for a total of N = 18 data sets with rates ranging from 0.6 to 19.6 CTCs per minute, or about 12 to 392 CTCs per mL of mouse blood.

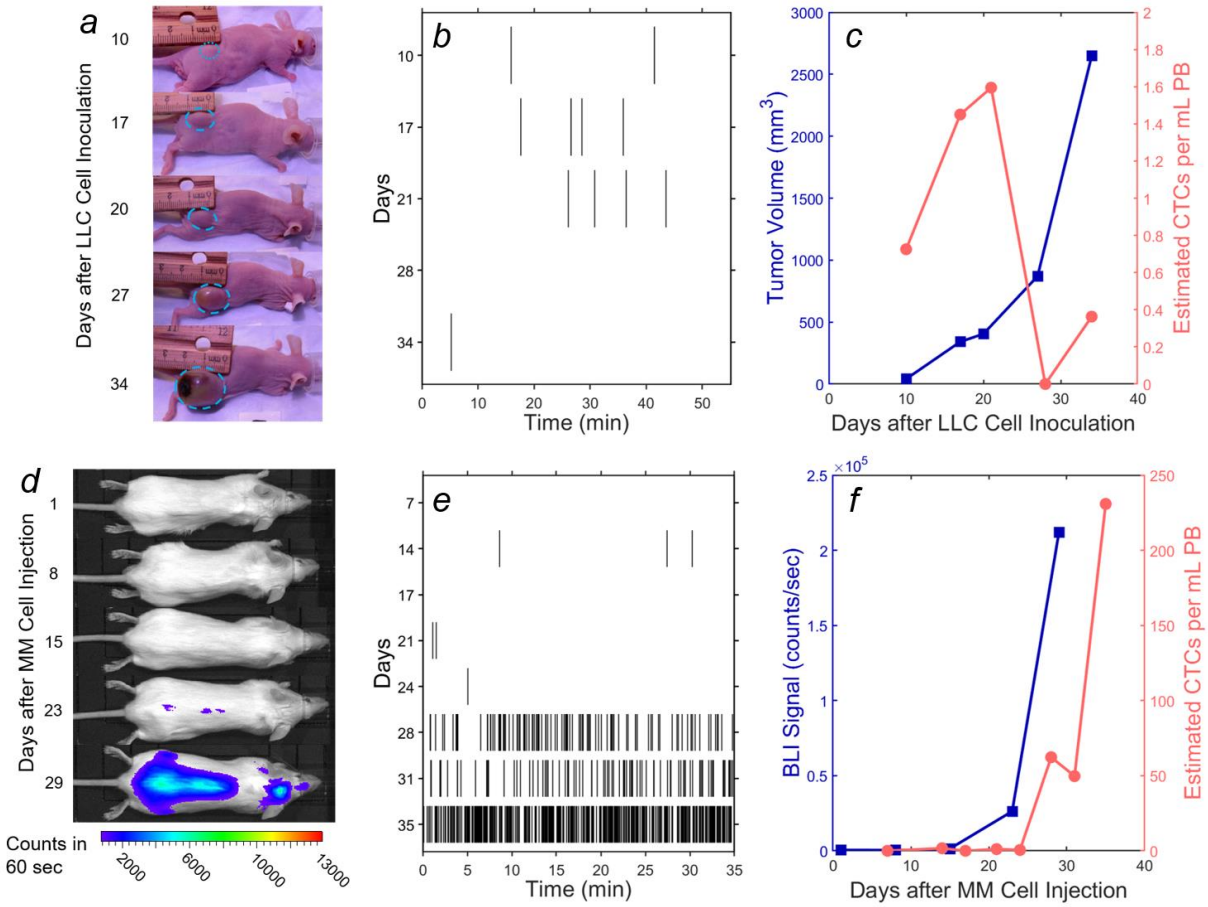

Figure 2. LLC Mouse (NRT3): (a) Pictures of tumor growth over the course of the experiment. (b) Raster plots of CTC detections of each scan of the same mouse. (c) Plot of the tumor volume (blue squares) and rate of CTC detections (pink circles) over time. MM Mouse (Cohort 2, Mouse 6): (d) BLI signal images of the mouse. (e) Raster plots of CTC detections. (f) Plot of BLI signal (blue squares) and rate of CTC detections (pink circles) over time.

iii) Microspheres in optical flow phantoms in vitro: We also used an optical flow phantom model with suspensions of fluorescent microspheres that were well-mixed, as we have done previously [30]. The rationale was to produce an experimental case where DiFC detections should follow Poisson statistics. Specifically, we used Dragon Green fluorescence level 5 (DG5) reference standard microspheres (Cat. DG06M, Bangs Laboratories, Inc., Fishers, IN) which have similar size and fluorescence intensity as a bright GFP-expressing cell. Microspheres were suspended in PBS at concentrations of approximately 200 and 400 μspheres per mL, and flowed through an optical phantom made from high-density polyethylene (HDPE) with similar optical properties of biological tissue. Tygon tubing (TGY-010-C, Small Parts, Inc., Seattle, WA) was threaded through a 1 mm diameter channel in the phantom centered at 0.75 mm from the surface and connected to a microsyringe pump (70-2209, Harvard Apparatus, Holliston, MA). Microspheres were pumped through the phantom at flow rates of 25, 50, and 100 μL/min, which produced linear flow speeds of 15, 30 and 60 mm/s, respectively. A clear matching gel (#875465, McKesson Medical-Surgical, Inc., Richmond, VA) was applied between the phantom surface and the DiFC probe tip to minimize laser light specular reflection. We performed DiFC for the 6 μsphere concentration and speed combinations yielding DiFC detection rates from 1.5 to 19.5 per minute. DiFC scanning was performed for 35 minutes in each case. Experiments were repeated in triplicate (N = 18 total data sets).

iv) Simulated DiFC data using Poisson statistics: We also simulated Poisson-distributed sequences of DiFC detections *in silico* as follows. The time between CTC detections follow an exponential distribution given by [15, 25]:

$$P(t\ seconds\ between\ CTCs) = \lambda_{seconds} e^{-t\lambda_{seconds}} \qquad (1)$$

Where $\lambda_{seconds}$ = DiFC scan average number of cells per second. We generated 35-minute data sets, where CTC detections were simulated in Matlab (The Mathworks Inc., Natick, MA) with an exponential random number generator with mean rates of detection ($\lambda_{seconds}$) equal to those of the MM and microsphere data sets, input 3 times each (N = 108 simulated scans).

Likewise, based on Poisson statistics, the probability of finding k CTCs in a blood sample, or the equivalent time interval of DiFC data, is expected to follow the distribution:

$$P(k) = \frac{{\lambda_T}^k e^{-\lambda_T}}{k!} \qquad (2)$$

Where, λ_T is the mean number of cells per blood sample (time interval). Note that $\lambda_T = T\lambda_{seconds}$ where T is the length of the respective time interval in seconds.

3. Results

3.1 Use of small equivalent blood samples frequently result in missed CTCs

We previously reported measurement of CTC numbers in blood in an LLC metastatic xenograft model [31]. We showed that while CTC count rate approximately correlated with the size of the primary tumor, significant day-to-day variability was observed and CTC numbers did not in general increase monotonically over time. Further analysis of our 60-minute DiFC scans in these mice showed that while pulmonary metastases were eventually observed in all cases, the DiFC count rate, and hence the number of CTCs in circulation at any given time was very low. This count rate could be directly related to the number of CTCs per mL of peripheral blood using the DiFC sampling rate of 50 μL of blood per minute. DiFC detection rates in this study ranged from 1.2 to 66 counts per hour, or approximately 0.4 to 22 CTCs per mL of blood. Example CTC-detection raster scans measured with DiFC are shown for LLC-bearing mice in **figures 3a-c,** where example data sets with relatively low, medium and high detection rates are shown.

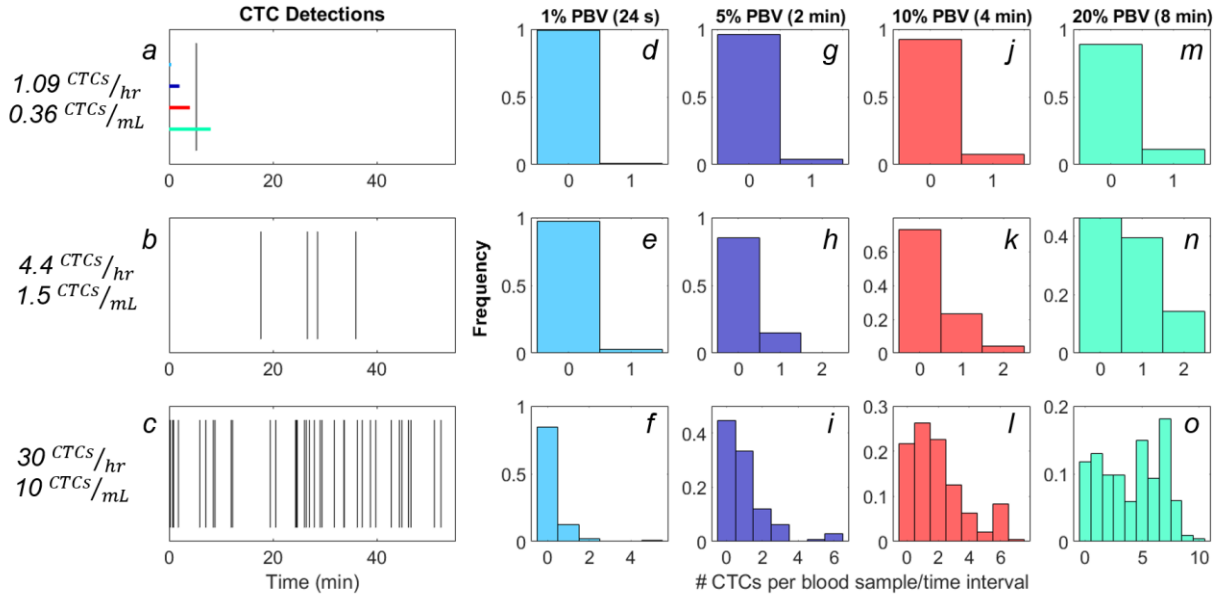

Figure 3. Raster plots (a-c) of LLC CTC detections at three different concentrations of CTCs in PB: (a) Low concentration ~ 0.36 CTCs/mL PB, (b) Medium concentration ~ 1.5 CTCs/mL PB, and (c) High concentration ~ 10 CTCs/mL PB. Colored horizontal lines illustrate the length of each time interval (blood sample size) relative to the DiFC scan length. Distributions of CTC counts from equivalent peripheral blood samples during these scans are shown: (d-f) 1% PBV samples (24 seconds of DiFC), (g-i) 5% PBV samples (2 minutes), (j-i) 10% PBV samples (4 minutes), and (m-o) 20% PBV samples (8 minutes).

Given these data, we consider the number of CTCs that would be detected in random 24s, 120s, 240s and 480s intervals, equivalent to approximately 1%, 5%, 10% and 20% of the mouse peripheral blood volume. Histograms of CTC detection frequency in the DiFC raster scans shown in ***figs. 3a-c*** are shown

for 24s (***figs. 3d-f***), 120s (***figs. 3g-i***), 240s (***figs.3 j-l***) and 480 s (***figs. 3m-o***) intervals, respectively. These data show that the probability that one or more CTCs were detected in a small temporal window was generally very low. For example, considering a 1% equivalent PBV with 0.5 CTCs per mL, zero CTCs would be detected in 99% of random blood draws over the scan duration. Even at a relatively high CTC burden of 10 CTCs per mL (***fig. 3c***), a 24s interval would yield zero CTC detections 89% of the time (***fig. 3f***). As might be expected, this probability was improved significantly for larger equivalent blood samples and for higher numbers of CTCs. For example, for a CTC burden of 10 CTCs per mL and an equivalent 20% PBV sample (***fig. 3o***), at least 1 CTC was detected 99% of the time.

The fraction of time intervals (equivalent blood samples) where at least 1 CTC was counted for all LLC mouse studies are shown in ***figure 4***. In combination these data underscore the fact that analysis of fractionally small (1-5% PBV) blood samples frequently resulted in detection of no CTCs, even when metastatic disease was present. Use of larger intervals significantly increased the likelihood of detection of at least 1 CTC. Hence these data provide direct animal model validation of the notion that 'more is better' for enumeration and analysis of CTCs [16].

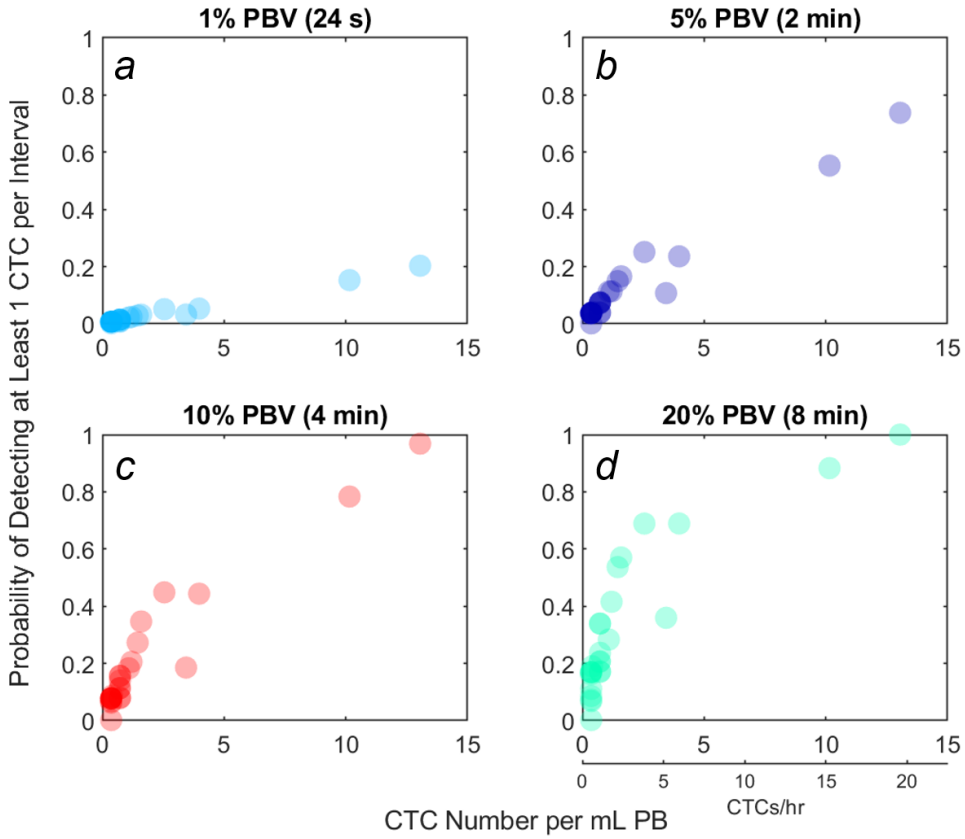

Figure 4. Probability of detecting 1 or more CTCs in a random blood sample (or the equivalent time interval of DiFC data) given that at least 1 CTC was detected in the DiFC scan. (a) 1% PBV samples (24 seconds), (b) 5% PBV samples (2 minutes), (c) 10% PBV samples (4 minutes), and (d) 20% PBV samples (8 minutes).

3.2 Estimating CTC numbers from small blood samples is quantitively inaccurate

We were also interested in the quantitative accuracy of CTC count from a fractionally small blood sample. To study this, we used data from our previously reported MM.1s disseminated mouse xenograft model, where CTCs were significantly more abundant [30]. Example data is shown in ***figure 5a***, which shows a 35-minute raster scan of CTC detections from an MM-bearing mouse, 28 days after engraftment of MM cells. The number of CTCs counted in moving 24, 120, 240 and 480s intervals are shown in ***figs. 5b-e***, respectively. As shown, the CTC counts vary significantly during the scan, with periods of relatively high and low CTC detection rates. As shown, we calculated the mean number of CTCs over the entire DiFC scan (black line), which we take to be the best estimate of the true CTC numbers during the scan period. The histograms of the number of CTC detections for all of the possible intervals (equivalent 1%, 5%, 10% and 20% PBV samples) in this DiFC scan are shown in ***fig. 5f-i,*** along with the mean number of CTCs detected over the entire scan (vertical black lines). This indicates the surprisingly large range of CTC detection rates over the 35-minute scan. For example, the CTC detection rates ranged from 0 to 41 CTCs per 120s interval (5% PBV), with a mean value over the scan of 18 CTCs. This data indicates that the number of CTCs counted in an equivalent blood sample drawn randomly during the scan could yield vastly different estimations of CTC numbers.

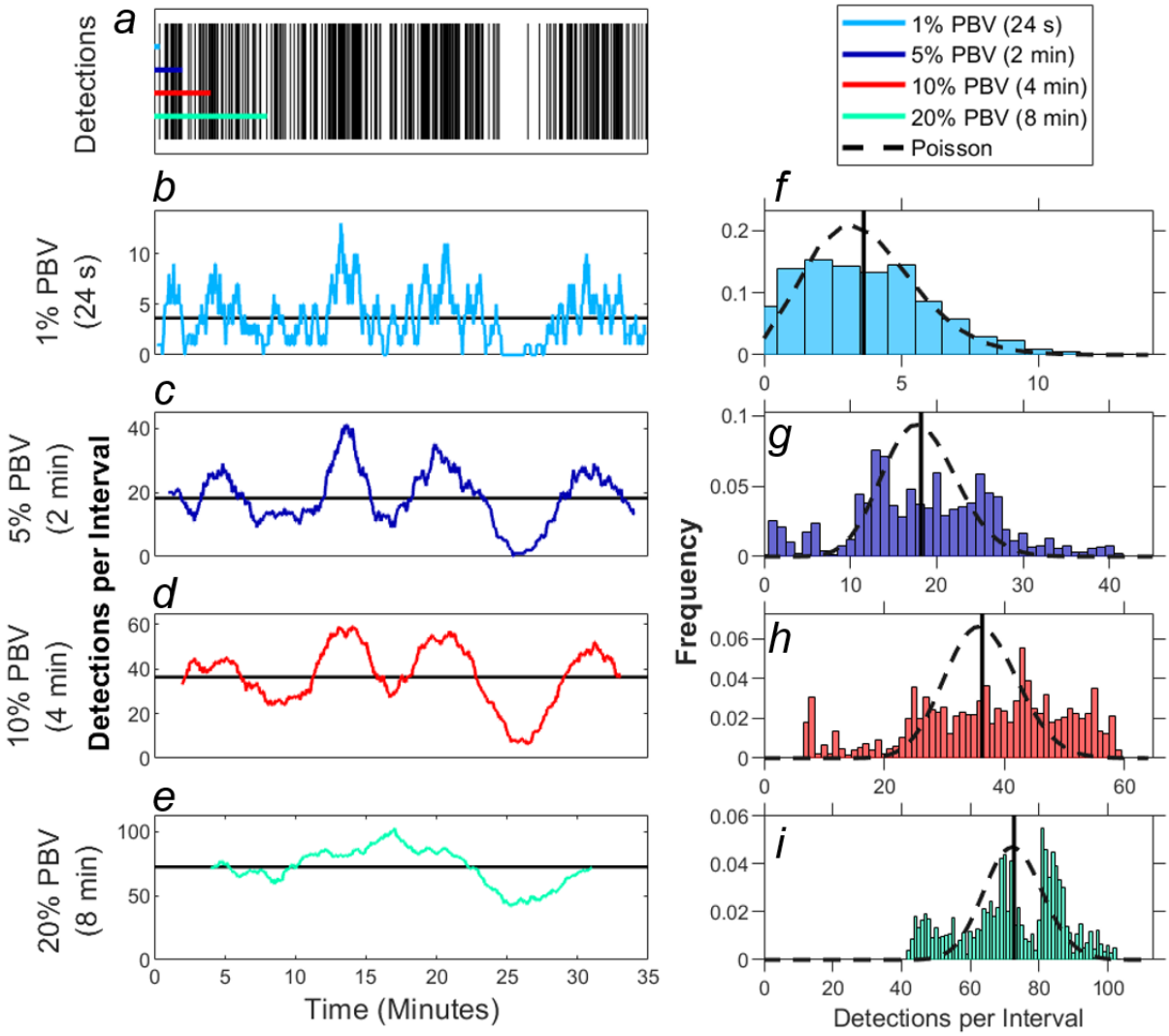

Figure 5. An example DiFC scan taken from a MM bearing mouse (Cohort 1, Mouse 3, Day 28): (a) Raster plot showing CTC detections in time. Colored horizontal lines demonstrate the length of each time interval (blood sample size) relative to the DiFC scan length. Plots of CTCs counted over (b) 1%, (c) 5%, (d) 10% and (e) 20% equivalent PBV samples. (f-i) Corresponding distributions of CTC counts per blood sample size. Expected distributions based on Poisson statistics are shown as dashed black lines.

We also compared these distributions to Poisson statistics which, as noted, are frequently assumed for CTC distributions in blood [15, 25, 34]. Specifically, we calculated the probability of *k* cells (***equation 2***) in an equivalent blood sample given the scan mean for each interval size (***figs. 5f-i***, dashed lines). By inspection, it can be seen that the DiFC-measured distribution of detection rates did not appear to follow the Poisson distributions, particularly for larger samples. The implications of this are discussed in more detail in section 3.3 below.

To better quantify the variability we observed, we also computed the deviation from the scan mean (DFSM) of the number of CTCs in each i_{th} equivalent sample (C_i) as:

$$DFSM_i = \frac{|C_i - \lambda_T|}{\lambda_T} * 100\% \quad (3)$$

where λ_T is the mean number of CTC detections over the full scan for each sample size.

We then considered the fraction of scan intervals (equivalent blood samples) where the DFSM was equal to or less than 25% and 50%. We did this for all 18 data sets we analyzed, as summarized in ***figure 6***. Use of 25% and 50% DFSM ranges are somewhat arbitrary, but are illustrative of sufficiently large error to affect decision making – for example in determining whether a sample has 4 or 5 CTCs (breast and prostate cancer) or 2 or 3 CTCs (colorectal cancer) [6, 17].

Taken together, these data show that quantitative estimation of CTC numbers from a single sample is extremely challenging. For example, for a scan interval of 120 s (5% PBV), the median probability of randomly obtaining a CTC count within 25% of the scan mean was only 40.8% (***fig. 6a***). Likewise, the probability of obtaining a CTC count within 50% of the mean was 72.3% (***fig. 6b***). Unsurprisingly, all else being equal, use of larger blood sample volumes yielded higher probability of obtaining accurate count than smaller samples [16].

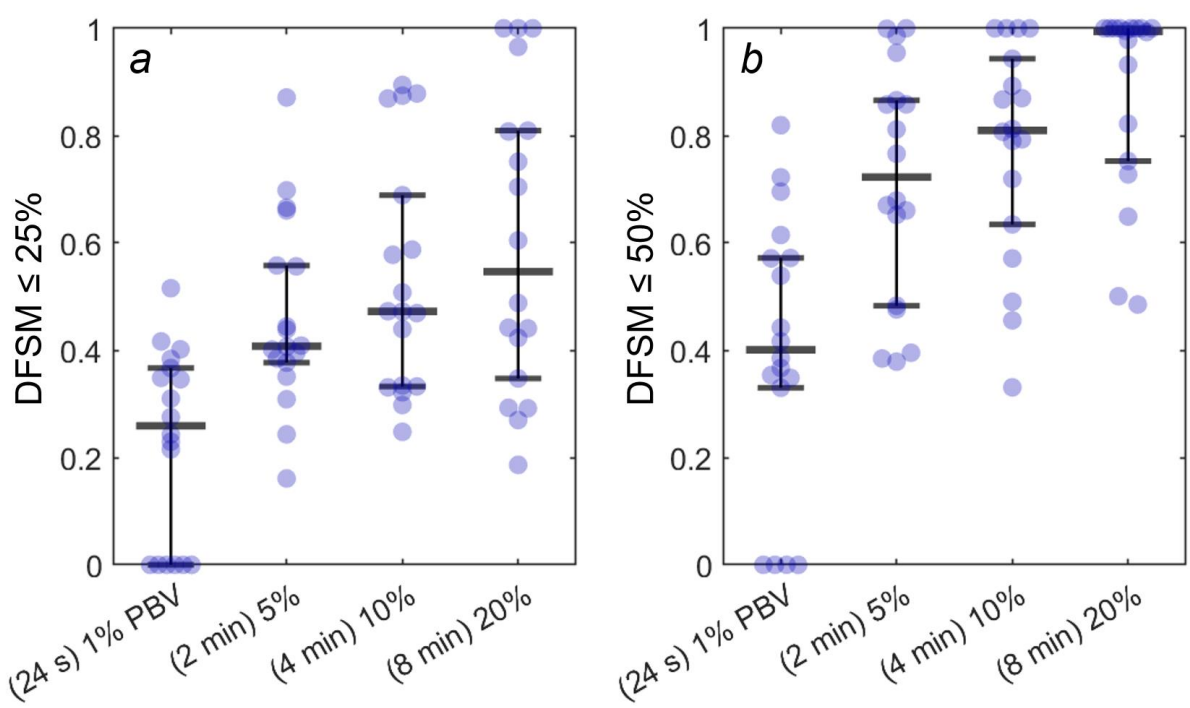

Figure 6. Generally, the counts in a small DiFC scan interval (equivalent blood sample) could vary significantly from the scan mean. The fraction of intervals with counts less than 25% and 50% deviation are shown for all data sets in our MM xenograft model. **(a)** Fraction of equivalent blood samples within +/-25% of the scan average concentration

of CTCs per blood sample (1% TBV: median = 0.259, range = 0 – 0.51.6; 5% TBV: median = 0.408, range = [0.161, 0.871]; 10% TBV: median = 0.472, range = [0.248, 0.895]; 20% TBV: median = 0.526, range = [0.186, 1.0]). **(b)** Fraction of samples within +/-50% (1% TBV: median = 0.401, range = [0, 0.819]; 5% TBV: median = 0.723, range =)0.379, 1.0]; 10% TBV: median = 0.832, range = [0.331, 1.0]; 20% TBV: median = 0.994, range = [0.485, 1.0]). Bars indicate the median, and first and third quartile for each case.

3.3 The variability in CTC detection rate was often higher than predicted by Poisson statistics

Because CTC detection is a random process, some variability of the measurements is naturally expected. However, the variability observed in the MM DXM data sets (for example in ***figure 5***) often appeared to exceed that predicted by Poisson statistics. As a simple illustration of this, we plotted the standard deviation of CTC counts against the square root of the mean (λ_T). This was repeated for 24, 120, 240 and 480 s intervals, for all 18 data sets. The results are shown in ***figs 7a-d***. As shown, the measured standard deviation was frequently higher than $\sqrt{\lambda_T}$.

To verify that this effect was not an artifact of the DiFC measurement or our data analysis approach, we repeated this analysis for simulated DiFC data where detections were Poisson distributed (**equation 1**) as shown in ***figs 7e-h***. We also performed DiFC measurements in a tissue-simulating optical flow phantom with suspensions of fluorescent microspheres that were well-mixed in solution as shown in ***figs. 7i-l***. In both cases, the standard deviation more closely agrees with the square root of the scan mean, as would be expected.

Based on this analysis, we next developed a test for whether the variability in CTC detection rates exceeded that predicted by Poisson statistics. For each data set, we calculated the fraction of observed time intervals with a number of CTCs within X% DFSM was calculated for X from 1% to 100% as shown in ***figs. 7m, n***. The equivalent curves predicted from Poisson statistics were also calculated as indicated by dotted lines in the plots. These were compared to the experimental measurements for 5%, 10%, and 20% PBV intervals at the 25% and 50% DFSM points and the sum of calculations from 1% to 100% DFSM (area under the curves in ***figs. 7m, n***). If the Poisson predictions were at least 15% larger than the experimental observations in a majority of these 9 comparisons, the data set was identified as "exceeds Poisson variability," otherwise it was identified as "consistent with Poisson."

Data sets meeting the definition of exceeding Poisson variability are plotted with red square markers in ***fig. 7***, whereas data sets that were consistent with Poisson statistics are plotted with blue markers. As shown, by this definition, 8 of 18 (44%) of MM xenograft data sets had variability exceeding Poisson statistics. On the other hand, only 1 of 108 (0.9%) of the simulated data sets and 1 of 18 (6%) of the phantom microsphere data sets by chance had exceeded Poisson variability. The main practical implication of the

result is that the likelihood of obtaining a quantitatively accurate CTC count from a single blood sample is actually worse than would be predicted by Poisson statistics for many of the in vivo data sets.

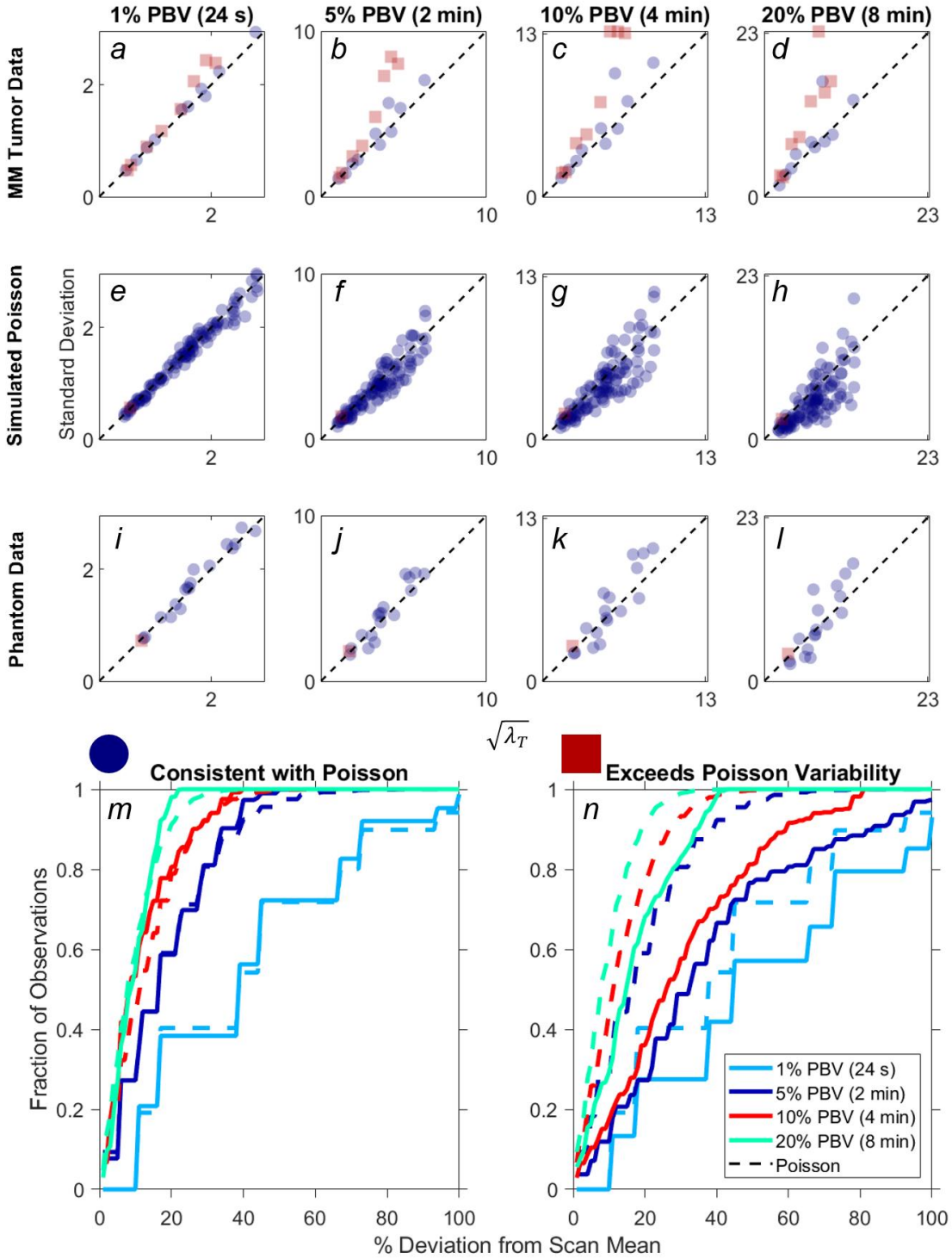

Figure 7. Comparison between the $\sqrt{\lambda_T}$ and the observed standard deviations: in vivo MM (a-d), simulations (e-h), and microspheres (i-l). Dotted lines show the 1:1 relationship that would be predicted from Poisson Statistics. Blue circles and red squares indicate data sets that are consistent with Poisson statistics and those that have greater variability than Poisson statistics, respectively. The fraction of observed time intervals with a number of CTCs within X% deviation from the scan mean was calculated from 1% to 100% for each data set. From these calculations, data sets were identified as either being consistent with Poisson or exceeding Poisson variability. Example MM DXM data sets for both cases are shown in (m) and (n), respectively.

3.4 Quantification of CTCs can be improved by averaging multiple samples

These data show that the mean number of detected CTCs varies significantly over the timescale of minutes, which further suggests that CTCs are not well-mixed in the peripheral blood. Likely physical explanations for this are discussed in more detail below. However, we hypothesized that based on this, averaging multiple small equivalent blood samples taken over the course of the scan should yield more accurate estimates of the true CTC count compared to a larger contiguous equivalent blood sample. For example, we compared five averaged 1% PBV measurements to a single 5% PBV measurement. For the former, we randomly sampled 3.96 million sets of five, 1% PBV samples from each MM DXM mouse data set.

The paired-difference (five 1% - 5%) in probability of obtaining a measurement with DFSM less than or equal to 25% and 50% are shown in ***figure 8***. While the median improvement in the two groups is 7.5% and 5.2%, respectively, in individual cases the improvement was as high as 32.6%. Moreover, when the data sets were separated into those that had variability exceeding Poisson statistics, the median improvements rose to 20.8% and 18.3%, respectively. As would be expected, for data sets where the variability was consistent with Poisson statistics, there was essentially no paired improvement (2.0% and -0.09%, respectively). These results suggest that, in addition to sampling more blood volume, improved accuracy in CTC enumeration (at least in our animal xenograft model) can be obtained by averaging several samples taken over longer periods of time.

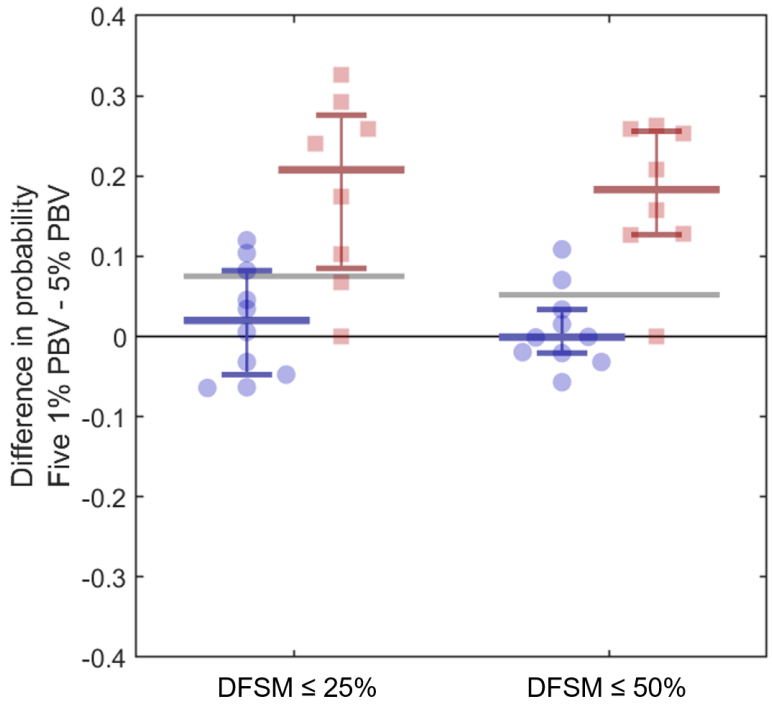

Figure 8. The difference in probabilities (Five 1% PBV – 5% PBV samples) of obtaining a CTC count result within 25% (left) and 50% (right) deviation from the scan mean (25%: median = 0.075; 50%: median = 0.052). Blue circles indicate data sets that are consistent with Poisson statistics (25%: median = 0.020, range = [-0.064, 0.120]; 50%: median = 0.0009, range = [-0.057, 0.108]). Red squares indicate data sets that have greater variability than Poisson statistics (25%: median = 0.208, range = [-0.0006, 0.327]; 50%: median = 0.183, range = [-.0006, 0.263]).

4. Discussion

Although CTCs are widely studied using liquid biopsy methods, their use of infrequent, fractionally small peripheral blood samples means that they are blind to natural temporal fluctuations in CTC numbers that occur over the timescale of minutes or hours. In contrast, in vivo methods of cell enumeration like DiFC uniquely allow measurement of these CTC dynamics. As we have noted, DiFC is unique amongst fluorescence-IVFC methods in that it allows enumeration of particularly rare cell populations.

Our analysis of two mouse xenograft models here shows that CTC numbers are highly dynamic over short timescales, and that any single small blood sample is unlikely to yield a quantitatively accurate picture of the CTC status in the mouse. For low CTC numbers (LLC model), it was most likely that a blood sample would not yield a single CTC detection, even considering samples up to 20% of the mouse PBV. For higher CTC numbers (MM model), a randomly selected blood sample up to 10% of the mouse PBV had less than 50% chance on average of yielding a CTC number estimate within 25% of the best estimate value. Although not directly comparable, as noted previously CTC assays like CellSearch analyze much less than 1% of the 5L human PBV.

DiFC data also suggests that CTCs may not be 'well-mixed' in the blood, meaning that the mean number of CTCs changes over time. It is well known that once shed into circulation, CTCs clear rapidly with a half-life of minutes or hours [19, 33, 35]. Previous DiFC and IVFC data are consistent with this [28, 36-40]. It has also been known for decades that tumors disseminate CTCs continuously at a rate of about 10^6 cells per gram of tumor tissue per day [41]. We were unable to find any specific published research on the short-term kinetics of CTC shedding into circulation, however it is possible or even likely that the rate of CTC shedding is not constant over the scale of minutes. For example, it has been shown that tumors cycle through hypoxia states on similar timescales [42]. The combination of short CTC half-life and non-constant CTC shedding from the tumor implies that CTCs are both being shed into and being cleared from circulation over short time scales, which would account for the short-term higher-than-anticipated variation in CTC numbers. CTC numbers may be better described using a 'bursty' kinetic model, analogous to burstiness in RNA transcription [43]. In one LLC data set analyzed in this paper, for example, only a single detection was observed in a 60-minute DiFC scan (e.g. ***fig. 3a***), suggesting that the CTC cleared from circulation before it could be detected a second time (which would have been likely given that DiFC would have sampled several mL of blood). We also performed DiFC in a LLC model for even longer periods (4 hours), as shown in figure 9, showing patterns of relatively high and low CTC activity.

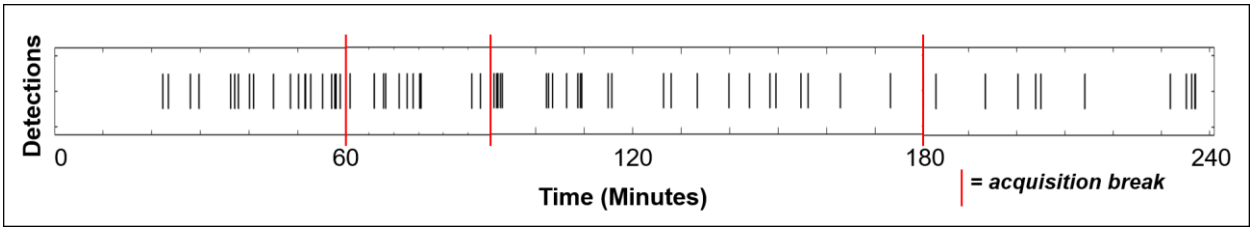

Figure 9. LLC CTC detections of a 4 hour DiFC scan, demonstrating periods of relatively high activity and inactivity. Red bars identify where the scan was interrupted for approximately 2 minutes to reapply clear matching gel to the mouse.

In practice, these data are consistent with the idea that improved CTC enumeration can be achieved by analysis of larger blood samples [15, 16], either by liquid biopsy or by using *in vivo* methods such as IVFC [44] or implantable CTC capture devices [45]. Moreover, our data suggest that in cases where the mean number of CTCs changes over time, averaging of multiple blood samples should yield better quantitative estimation of CTC numbers than a single larger blood sample. The high-degree of CTC turnover in peripheral blood also suggests that anti-CTC therapeutic strategies such as so-called "CTC dialysis" [46, 47] are unlikely to succeed unless performed continuously.

Last, we acknowledge that these observations are made from two mouse models of cancer with immortalized cell lines. Whether these observations extend to other mouse models, or to human cancers is not yet known. However, these data are generally consistent with the small number of previous IVFC studies of short-term CTC numbers in mice [32]. "Spaghetti plots" of CTC numbers taken over time in human patients also suggest significant variation [48]. It is plausible that human cancers behave even more heterogeneously than mouse xenograft models. Extension of this work to other animal models of metastasis, and better modeling of CTC kinetics is the subject of ongoing research in our group.

References

1. Gupta, G.P. and J. Massague, *Cancer metastasis: building a framework.* Cell, 2006. **127**(4): p. 679-95.
2. Steeg, P.S. and D. Theodorescu, *Metastasis: a therapeutic target for cancer.* Nat Clin Pract Oncol, 2008. **5**(4): p. 206-19.
3. Alix-Panabieres, C. and K. Pantel, *Circulating tumor cells: liquid biopsy of cancer.* Clin Chem, 2013. **59**(1): p. 110-8.
4. Mader, S. and K. Pantel, *Liquid Biopsy: Current Status and Future Perspectives.* Oncol Res Treat, 2017. **40**(7-8): p. 404-408.
5. Cristofanilli, M., et al., *Circulating tumor cells, disease progression, and survival in metastatic breast cancer.* N Engl J Med, 2004. **351**(8): p. 781-91.
6. Cohen, S.J., et al., *Relationship of circulating tumor cells to tumor response, progression-free survival, and overall survival in patients with metastatic colorectal cancer.* J Clin Oncol, 2008. **26**(19): p. 3213-21.
7. Moreno, J.G., et al., *Circulating tumor cells predict survival in patients with metastatic prostate cancer.* Urology, 2005. **65**(4): p. 713-8.
8. Smerage, J.B., et al., *Circulating tumor cells and response to chemotherapy in metastatic breast cancer: SWOG S0500.* J Clin Oncol, 2014. **32**(31): p. 3483-9.
9. Raimondi, C., et al., *Clinical utility of circulating tumor cell counting through CellSearch((R)): the dilemma of a concept suspended in Limbo.* Onco Targets Ther, 2014. **7**: p. 619-25.
10. Toss, A., et al., *CTC enumeration and characterization: moving toward personalized medicine.* Ann Transl Med, 2014. **2**(11): p. 108.
11. Alix-Panabieres, C. and K. Pantel, *Challenges in circulating tumour cell research.* Nat Rev Cancer, 2014. **14**(9): p. 623-31.
12. Li, Y., S. Wu, and F. Bai, *Molecular characterization of circulating tumor cells-from bench to bedside.* Semin Cell Dev Biol, 2018. **75**: p. 88-97.
13. Hwang, W.L., H.M. Pleskow, and D.T. Miyamoto, *Molecular analysis of circulating tumors cells: Biomarkers beyond enumeration.* Adv Drug Deliv Rev, 2018. **125**: p. 122-131.
14. Polzer, B., et al., *Molecular profiling of single circulating tumor cells with diagnostic intention.* EMBO Mol Med, 2014. **6**(11): p. 1371-86.
15. Allan, A.L. and M. Keeney, *Circulating tumor cell analysis: technical and statistical considerations for application to the clinic.* J Oncol, 2010. **2010**: p. 426218.
16. Lalmahomed, Z.S., et al., *Circulating tumor cells and sample size: the more, the better.* J Clin Oncol, 2010. **28**(17): p. e288-9; author reply e290.
17. Hayes, D.F., et al., *Circulating tumor cells at each follow-up time point during therapy of metastatic breast cancer patients predict progression-free and overall survival.* Clin Cancer Res, 2006. **12**(14 Pt 1): p. 4218-24.
18. de Bono, J.S., et al., *Circulating tumor cells predict survival benefit from treatment in metastatic castration-resistant prostate cancer.* Clin Cancer Res, 2008. **14**(19): p. 6302-9.
19. Stott, S.L., et al., *Isolation and characterization of circulating tumor cells from patients with localized and metastatic prostate cancer.* Sci Transl Med, 2010. **2**(25): p. 25ra23.
20. Karabacak, N.M., et al., *Microfluidic, marker-free isolation of circulating tumor cells from blood samples.* Nat Protoc, 2014. **9**(3): p. 694-710.
21. Au, S.H., et al., *Microfluidic Isolation of Circulating Tumor Cell Clusters by Size and Asymmetry.* Sci Rep, 2017. **7**(1): p. 2433.
22. Hoff, J., *Methods of blood collection in the mouse.* Lab Animal, 2000. **29**(10): p. 47-53.
23. Hartmann, C., et al., *Fluorescence detection, enumeration and characterization of single circulating cells in vivo: technology, applications and future prospects.* Phys Med Biol, 2017. **63**(1): p. 01TR01.
24. Maestro, L.M., et al., *Circulating tumor cells in solid tumor in metastatic and localized stages.* Anticancer Res, 2009. **29**(11): p. 4839-43.
25. Tibbe, A.G., M.C. Miller, and L.W. Terstappen, *Statistical considerations for enumeration of circulating tumor cells.* Cytometry A, 2007. **71**(3): p. 154-62.
26. Tuchin, V.V., A. Tarnok, and V.P. Zharov, *In vivo flow cytometry: a horizon of opportunities.* Cytometry A, 2011. **79**(10): p. 737-45.

27. Zettergren, E., et al., *Instrument for fluorescence sensing of circulating cells with diffuse light in mice in vivo.* J Biomed Opt, 2012. **17**(3): p. 037001.
28. Pera, V., et al., *Diffuse fluorescence fiber probe for in vivo detection of circulating cells.* J Biomed Opt, 2017. **22**(3): p. 37004.
29. Tan, X., et al., *In Vivo Flow Cytometry of Extremely Rare Circulating Cells.* Sci Rep, 2019. **9**(1): p. 3366.
30. Patil, R., et al., *Fluorescence monitoring of rare circulating tumor cell and cluster dissemination in a multiple myeloma xenograft model in vivo.* J Biomed Opt, 2019. **24**(8): p. 1-11.
31. Fitzgerald, J., R. Patil, and M. Niedre, *Monitoring of Circulating Tumor Cell and Cluster Dissemination in a Metastic Lewis Lung Carcinoma Model in Mice.* In preparation.
32. Juratli, M.A., et al., *Dynamic Fluctuation of Circulating Tumor Cells during Cancer Progression.* Cancers (Basel), 2014. **6**(1): p. 128-42.
33. Meng, S., et al., *Circulating tumor cells in patients with breast cancer dormancy.* Clin Cancer Res, 2004. **10**(24): p. 8152-62.
34. Coumans, F.A., S.T. Ligthart, and L.W. Terstappen, *Interpretation of changes in circulating tumor cell counts.* Transl Oncol, 2012. **5**(6): p. 486-91.
35. Aceto, N., et al., *Circulating tumor cell clusters are oligoclonal precursors of breast cancer metastasis.* Cell, 2014. **158**(5): p. 1110-1122.
36. Georgakoudi, I., et al., *In vivo flow cytometry: a new method for enumerating circulating cancer cells.* Cancer Res, 2004. **64**(15): p. 5044-7.
37. Sipkins, D.A., et al., *In vivo imaging of specialized bone marrow endothelial microdomains for tumour engraftment.* Nature, 2005. **435**(7044): p. 969-73.
38. He, W., et al., *In vivo quantitation of rare circulating tumor cells by multiphoton intravital flow cytometry.* Proc Natl Acad Sci U S A, 2007. **104**(28): p. 11760-5.
39. Runnels, J.M., et al., *Optical techniques for tracking multiple myeloma engraftment, growth, and response to therapy.* J Biomed Opt, 2011. **16**(1): p. 011006.
40. Pestana, N., et al., *Improved diffuse fluorescence flow cytometer prototype for high sensitivity detection of rare circulating cells in vivo.* J Biomed Opt, 2013. **18**(7): p. 077002.
41. Butler, T.P. and P.M. Gullino, *Quantitation of cell shedding into efferent blood of mammary adenocarcinoma.* Cancer Res, 1975. **35**(3): p. 512-6.
42. Dewhirst, M.W., *Relationships between cycling hypoxia, HIF-1, angiogenesis and oxidative stress.* Radiat Res, 2009. **172**(6): p. 653-65.
43. Corrigan, A.M., et al., *A continuum model of transcriptional bursting.* Elife, 2016. **5**.
44. Galanzha, E.I., et al., *In vivo liquid biopsy using Cytophone platform for photoacoustic detection of circulating tumor cells in patients with melanoma.* Sci Transl Med, 2019. **11**(496).
45. Saucedo-Zeni, N., et al., *A novel method for the in vivo isolation of circulating tumor cells from peripheral blood of cancer patients using a functionalized and structured medical wire.* Int J Oncol, 2012. **41**(4): p. 1241-50.
46. Faltas, B., *Cornering metastases: therapeutic targeting of circulating tumor cells and stem cells.* Front Oncol, 2012. **2**: p. 68.
47. Kim, Y.R., et al., *Selective killing of circulating tumor cells prevents metastasis and extends survival.* J Hematol Oncol, 2018. **11**(1): p. 114.
48. Wilbaux, M., et al., *A Joint Model for the Kinetics of CTC Count and PSA Concentration During Treatment in Metastatic Castration-Resistant Prostate Cancer.* CPT Pharmacometrics Syst Pharmacol, 2015. **4**(5): p. 277-85.